Structures and photophysical properties of 3,4-diaryl-1H-pyrrol-2,5-diimines and 2,3-diarylmaleimides

Afanasenko, Anastasiia M.; Boyarskaya, Dina V.; Boyarskaya, Irina A.; Chulkova, Tatiana G.; Grigoriev, Yakov M.; Kolesnikov, Ilya E.; Avdontceva, Margarita S.; Panikorovskii, Taras L.; Panin, Andrej I.; Vereshchagin, Anatoly N.

Published in:
Journal of Molecular Structure

DOI:
10.1016/j.molstruc.2017.06.048

Publication date:
2017

Journal of Molecular Structure 1146 (2017) 554–561

Contents lists available at ScienceDirect

Journal of Molecular Structure

journal homepage: http://www.elsevier.com/locate/molstruc

Structures and photophysical properties of 3,4-diaryl-1*H*-pyrrol-2,5-diimines and 2,3-diarylmaleimides

Anastasiia M. Afanasenko [a, b], Dina V. Boyarskaya [a], Irina A. Boyarskaya [a], Tatiana G. Chulkova [a, *], Yakov M. Grigoriev [a], Ilya E. Kolesnikov [a], Margarita S. Avdontceva [a], Taras L. Panikorovskii [a], Andrej I. Panin [a], Anatoly N. Vereshchagin [c], Michail N. Elinson [c]

[a] Saint Petersburg State University, 7/9 Universitetskaya Nab., Saint Petersburg, 199034, Russia
[b] Stratingh Institute for Chemistry, University of Groningen, Nijenborgh 4, 9747 AG, Groningen, The Netherlands
[c] N. D. Zelinsky Institute of Organic Chemistry, 47 Leninsky Prospect, Moscow, 119991, Russia

ARTICLE INFO

Article history:
Received 16 January 2017
Received in revised form
11 June 2017
Accepted 12 June 2017
Available online 13 June 2017

Keywords:
2,3-Diarylmaleimides
3,4-Diaryl-1*H*-pyrrol-2,5-diimines
DFT and TD-DFT studies
Fluorescence

ABSTRACT

Structural features of 3,4-diaryl-1*H*-pyrrol-2,5-diimines and their derivatives have been studied by molecular spectroscopy techniques, single-crystal X-ray diffraction, and DFT calculations. According to the theoretical calculations, the diimino tautomeric form of 3,4-diaryl-1*H*-pyrrol-2,5-diimines is more stable in solution than the imino-enamino form. We also found that the structurally related 2,3-diarylmaleimides exist in the solid state in the dimeric diketo form. 3,4-Diaryl-1*H*-pyrrol-2,5-diimines and 2,3-diarylmaleimides exhibit fluorescence in the blue region of the visible spectrum. The fluorescence spectra have large Stokes shifts. Aryl substituents at the 3,4-positions of 1*H*-pyrrol-2,5-diimine do not significantly affect fluorescence properties. The insertion of donor substituents into 2,3-diarylmaleimides leads to bathochromic shift of emission bands with hyperchromic effect.

1. Introduction

In recent years, organic fluorescent compounds have attracted considerable attention as objects for the basic research and commercial applications [1–3]. These substances are useful in organic light-emitting diodes (OLEDs), fluorimetric sensors, surface coatings, inks, cosmetics, and textile industries. No reports on fluorescence properties of pyrrol-2,5-diimines were published until this work, however, optical properties of some of their derivatives were studied both experimentally and theoretically [4–6]. Most of the species in the dicarboxylic acid imide family, such as phthalimide, naphthalimide, and perylenebisimide have been generated for their UV–vis absorption or fluorescence property [7,8]. Recently, Chen et al. reported the first bright and efficient non-doped red organic emitting diode based on naphthylphenylamino-substituted *N*-methyl-2,3-diphenylmaleimide as the host emitter, which is a deep red fluorophore with a relatively large Stokes shift both in solution and the solid phase [9]. Chen et al. also reported on a new synthesis procedure for a series of 2,3-diarylmaleimide based fluorophores, where the aryl substituent could be phenyl, 1-naphthyl, 2-naphthyl, etc. carrying varied functionality [8]. It is known, that 2,3-diarylsubstituted maleimide compounds also behave as fluorophores with various colors of fluorescence and exhibit larger Stokes shift in more polar solvents [10,11].

In this work, we studied structures and photophysical properties of 3,4-diaryl-1*H*-pyrrol-2,5-diimines and 2,3-diarylmaleimides. Tautomerizm, conformations, non-covalent intermolecular interactions and their influence on optic properties of these compounds are in the focus of our investigation.

2. Experimental

2.1. Materials and methods

All solvents were dried and purified by conventional methods and were freshly distilled under argon shortly before use. Other reagents were used without further purification. FTIR spectra were recorded on Shimadzu FTIR-8400S (4000–400 cm^{-1}) and IRAffinity-1 (4000–350 cm^{-1}) spectrometers using KBr pellets. ^1H

* Corresponding author.
E-mail address: t.chulkova@spbu.ru (T.G. Chulkova).

http://dx.doi.org/10.1016/j.molstruc.2017.06.048
0022-2860/

NMR measurements were performed on a Bruker-DPX 400 instrument at ambient temperature. Electrospray ionization mass spectra were obtained on a Bruker micrOTOF spectrometer equipped with electrospray ionization (ESI) source using MeOH as the solvent. The instrument was operated in both positive and negative ion modes using a *m*/*z* range of 50–3000. The capillary voltage of the ion source was set at −4500 V (ESI^+–MS) or 3500 V (ESI^+–MS) and the capillary exit at ±(70–150) V. The nebulizer gas flow was 0.4 bar and drying gas flow 4.0 L/min. The absorption spectra were recorded on a Perkin–Elmer precision spectrophotometer Lambda 1050. The emission spectra, excitation spectra, measurements of the lifetimes of excited states were measured on a modular spectrofluorimeter Fluorolog-3 (Horiba Jobin Yvon). Fluorescence lifetime measurements are based on time-correlated single photon counting (TCSPC). Device also includes an integrating sphere Quanta-φ with fiber optics which enables direct measurement of quantum yields of luminescence.

2.2. Synthetic procedures

3,4-Diaryl-1*H*-pyrrol-2,5-diimines **2a**–**f** were obtained from the appropriate commercially available arylacetonitriles by two step reaction. The synthetic scheme is shown in Fig. 1. Starting from a series of arylacetonitriles, following Linstead's procedure [12], yielded the nitriles of 2,3-diarylbutenedioic acids **1a**–**d**. 2,3-Diarylfumaronitriles **1e** and **1f** were produced electrochemically from the appropriate arylacetonitriles [13]. Compounds **1a**–**f** were converted to the corresponding 3,4-diaryl-*1H*-pyrrol-2,5-diimines **2a**–**f** by bubbling of dry ammonia into ethylene glycol solution [14].

3,4-Diphenyl-1H-pyrrol-2,5-diimine (**2a**): Yield 0.480 g (89%). ^1H NMR spectrum (300 MHz, $CDCl_3$) δ, ppm: 7.43–7.35 (m, 6 H, H–Ar), 7.27–7.19 (m, 4H, H–Ar). $^{13}C\{^1H\}$ NMR spectrum (100 MHz, $CDCl_3$) δ, ppm: 166.2 (C=N), 129.6, 129.4, 129.1, 128.9, 128.3. IR spectrum (KBr, selected bands, cm^{-1}): 1659 s ν(C=N). HRMS (ESI^+), *m*/*z*: 248.1181 $[M+H]^+$, 495.2234 $[2M+H]^+$. $C_{16}H_{14}N_3$. Calcd., *m*/*z*: 248.1188.

3,4-Di(4-methylphenyl)-1H-pyrrol-2,5-diimine (**2b**): Yield 0.476 g (91%). ^1H NMR spectrum (400 MHz, $CDCl_3$) δ, ppm: 7.19 (d, ^3J = 9.0 Hz, 4H, H–Ar), 7.13 (d, ^3J = 9.0 Hz, 4H, H–Ar), 2.37 (s, 6H, CH_3). $^{13}C\{^1H\}$ NMR spectrum (100 MHz, $CDCl_3$) δ, ppm: 166.6 (=C), 139.1 (C^p), 129.9, 129.6 (CH), 128.6 (CH), 127.0, 21.4 (CH_3). IR spectrum (KBr, selected bands, cm^{-1}): 1641 s ν(C=N), 1535 *m* ν(CCAr). HRMS (ESI^+), *m*/*z*: 276.1504 $[M+H]^+$. $C_{18}H_{18}N_3$. Calcd., *m*/*z*: 276.1501.

3,4-Di(4-methoxyphenyl)-1H-pyrrol-2,5-diimine (**2c**) [15]: Yield 0.493 g (94%). ^1H NMR spectrum (400 MHz, $CDCl_3$) δ, ppm: 7.82 (d, ^3J = 9.0 Hz, 4H, H–Ar), 7.04 (d, ^3J = 9.0 Hz, 4H, H–Ar), 3.91 (s, 6H, CH_3). $^{13}C\{^1H\}$ NMR spectrum (100 MHz, $CDCl_3$) δ, ppm: 166.7, 160.1, 130.8, 122.1, 122.0, 114.5, 55.3 (OCH_3). IR spectrum (KBr, selected bands, cm^{-1}): 1647 s ν(C=N), 1605 s, 1504 s ν(CCAr). HRMS (ESI^+), *m*/*z*: 308.1402 $[M+H]^+$. $C_{18}H_{18}N_3O_2$. Calcd., *m*/*z*: 308.1399.

3,4-Di(4-fluorophenyl)-1H-pyrrol-2,5-diimine (**2d**): Yield 0.432 g (81%). ^1H NMR spectrum (400 MHz, $CDCl_3$) δ, ppm: 7.23 (m, 4H, H–Ar), 7.11 (d, ^3J = 8.0 Hz, 2H, H–Ar), 7.08 (d, ^3J = 8.0 Hz, 2H, H–Ar). $^{13}C\{^1H\}$ NMR spectrum (100 MHz, $CDCl_3$) δ, ppm: 165.3 ($^1J_{CF}$ = 189.0 Hz, C^p), 161.9 (=C), 131.9 (C^{ipso}), 131.4 ($^3J_{CF}$ = 8.0 Hz, C^o), 125.6 (C=C), 116.3 ($^2J_{CF}$ = 22.0 Hz, C^m). IR spectrum (KBr, selected bands, cm^{-1}): 1643 s ν(C=N), 1601 s, 1502 s ν(CCAr). HRMS (ESI^+), *m*/*z*: 284.0998 $[M+H]^+$. $C_{16}H_{12}N_3F_2$. Calcd., *m*/*z*: 284.0999.

3,4-Di(4-chlorophenyl)-1H-pyrrol-2,5-diimine (**2e**): Yield 0.424 g (81%). ^1H NMR spectrum (400 MHz, $CDCl_3$) δ, ppm: 7.39 (d, ^3J = 8.0 Hz, 4H, H–Ar), 7.18 (d, ^3J = 8.0 Hz, 4H, H–Ar). $^{13}C\{^1H\}$ NMR spectrum (100 MHz, $CDCl_3$) δ, ppm: 166.2 (C=N), 135.7, 130.7, 129.5 (CH), 128.0 (CH), 128.0. IR spectrum (KBr, selected bands, cm^{-1}): 1645 s ν(C=N), 1593, 1483 *m* ν(CCAr). HRMS (ESI^+), *m*/*z*: 316.0391 $[M+H]^+$. $C_{16}H_{12}N_3Cl_2$. Calcd., *m*/*z*:. 316.0408.

3,4-Di(4-bromophenyl)-1H-pyrrol-2,5-diimine (**2f**) [15]: Yield 0.438 g (83%). ^1H NMR spectrum (400 MHz, $CDCl_3$) δ, ppm: 7.55 (d, ^3J = 8.0 Hz, 4H, H–Ar), 7.11 (d, ^3J = 8.0 Hz, 4H, H–Ar). $^{13}C\{^1H\}$ NMR spectrum (100 MHz, $CDCl_3$) δ, ppm: 166.1 (C=N), 132.4, 131.9 (CH), 130.9 (CH), 128.4, 124.0. IR spectrum (KBr, selected bands, cm^{-1}): 1645 s ν(C=N), 1533, 1479 *m* ν(CCAr). HRMS (ESI^+), *m*/*z*: 509.8365 $[M+Ag]^+$. $C_{16}H_{11}N_3Br_2Ag$. Calcd., *m*/*z*: 509.8371.

2,3-Diarylmaleimides **3a**–**d** were synthesized by hydrolysis of 3,4-diaryl-1*H*-pyrrol-2,5-diimines in aqueous methanol [16]. These compounds were prepared with quantitative yields. Crystals of **3b**–**d** suitable for X-ray diffraction were grown from a concentrated chloroform solution.

2,3-Diphenylmaleimide (**3a**): ^1H NMR spectrum of the compound is identical to previously published data [17].

2,3-Di(4-methylphenyl)maleimide (**3b**): ^1H NMR spectrum (400 MHz, $CDCl_3$) δ, ppm: 7.86 (s, 2H, NH), 7.41 (d, *J* = 8.00 Hz, 8H, Ar), 7.19 (d, *J* = 8.00 Hz, 8H, Ar), 2.39 (s, 12H, CH_3). $^{13}C\{^1H\}$ NMR spectrum (100 MHz, $CDCl_3$) δ, ppm: 170.8, 140.2, 136.4, 129.8, 129.3, 125.6, 21.5. IR (KBr, selected bands, cm^{-1}): 1713 s ν(C=O), 1607, 1503 *m* ν(CCAr). HRMS (ESI^+), *m*/*z*: 277.1341 $[M+H]^+$ (calc. 277.1103), 300.1005 $[M+Na]^+$ (calc. 300.1000), 577.2118 $[2M+Na]^+$ (calc. 577.2103).

2,3-Di(4-methoxyphenyl)maleimide (**3c**): ^1H NMR spectrum (400 MHz, $CDCl_3$) δ, ppm: 7.40 (s, 2H, NH), 7.50 (d, *J* = 8.00 Hz, 8H, Ar), 6.91 (d, *J* = 8.00 Hz, 8H, Ar), 3.86 (s, 6H, CH_3O). $^{13}C\{^1H\}$ NMR spectrum (100 MHz, $CDCl_3$) δ, ppm: 170.7, 160.8, 135.0, 131.5, 121.1, 114.1, 55.3. IR spectrum (KBr, selected bands, cm^{-1}): 1707 s ν(C=O), 1601 *m*, 1516 *m* ν(CCAr). HRMS (ESI^+), *m*/*z*: 332.0888 $[M+Na]^+$ (calc. 332.0899), 641.1889 $[2M+Na]^+$ (calc. 641.1899).

2,3-Di(4-fluorophenyl)maleimide (**3d**): ^1H NMR spectrum (400 MHz, $CDCl_3$) δ, ppm: 7.88 (s, 2H, NH), 7.51 (d, *J* = 8.00 Hz, 4H, Ar), 7.48 (d, *J* = 8.00 Hz, 4H, Ar), 7.105 (d, *J* = 12.00 Hz, 4H, Ar), 7.075

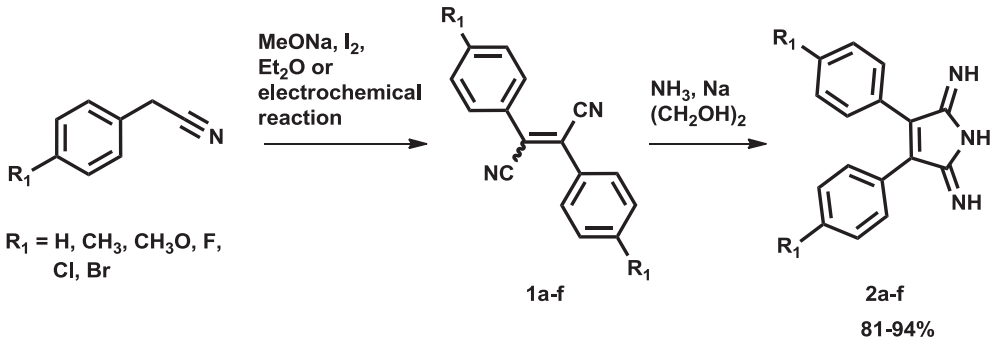

Fig. 1. Preparation of 3,4-diaryl-1*H*-pyrrol-2,5-diimines **2a**–**f**.

(d, J = 12.00 Hz, 4H, Ar). $^{13}C\{^1H\}$ NMR spectrum (100 MHz, $CDCl_3$) δ, ppm: 170.1, 164.9, 162.4, 135.8, 132.0, 131.9, 124.2, 116.2, 116.0. IR spectrum (KBr, selected bands, cm^{-1}): 1710 s ν(C=O), 1599, 1503 *m* ν(CCAr). HRMS (ESI^+), *m/z*: 308.0504 $[M+Na]^+$ (calc. 308.0499), 555.5091 $[2M+Na]^+$ (calc. 555.1132).

2.3. Crystallography

The crystals of **3b**–**d** were obtained by a slow evaporation of solvent at room temperature. Crystals of compounds **3b**–**d** were immersed in cryo-oil, mounted in a nylon loop, and analyzed at a temperature of 100 K. The X-ray diffraction data were collected on an Agilent Technologies Excalibur Eos and Supernova Atlas diffractometers. The temperature for all experiments was kept at 100 K. The structures have been solved by the direct methods and refined by means of the SHELXL–97 [18] program incorporated in the $OLEX^2$ program package [19]. The carbon-bound H atoms were placed in calculated positions and were included in the refinement in the 'riding' model approximation, with $U_{iso}(H)$ set to $1.5U_{eq}(C)$ and C–H 0.96 Å for CH_3 groups, $U_{iso}(H)$ set to $1.2U_{eq}(C)$ and C–H 0.93 Å for the CH groups, and $U_{iso}(H)$ set to $1.2U_{eq}(N)$ and N–H 0.86 Å for the NH groups. Empirical absorption correction was applied in CrysAlisPro program complex [20] using spherical harmonics, implemented in SCALE3 ABSPACK scaling algorithm.

The crystallographic details and refinement parameters are summarized in Table 1. The crystal structures and crystallographic details are given in Figs. S1–S3 and Tables S1–S4 of the Supporting Information. Crystal data have been deposited at the Cambridge Crystallographic Data Centre (CCDC) with deposition numbers CCDC 1518210, CCDC 1518077, and CCDC 1518211 for **3b**, **3c**, and **3d**, respectively.

2.4. Computational details

The full geometry optimization, orbital views, orbital energies, total energies, electron transitions in the UV–vis spectra have been carried out at the DFT hybrid level of theory using Becke's three-parameter hybrid exchange functional in combination with the gradient-corrected correlation functional of Lee, Yang, and Parr (B3LYP) [21–24] and standard basis 6-31+G (d,p) in methanol using the Gaussian 03 [25] (if not explicitly stated otherwise) and Gaussian 09 [26] program packages. The relative energies of pyrroldiimine (or maleimide) dimerization were calculated per one molecule of pyrroldiimine (or maleimide).

Table 1
Crystallographic data and refinement parameters.

	3b dimer	3c dimer	3d dimer
Empirical formula	$C_{36}H_{30}N_2O_4$	$C_{36}H_{30}N_2O_8$	$C_{32}H_{18}N_2O_4F_4$
Molecular weight	554.62	618.63	570.48
Temp (K)	100 (2)	100 (2)	100 (2)
Radiation	CuKα	CuKα	MoKα
Crystal system	Triclinic	Triclinic	Monoclinic
Space group	*P*-1	*P*-1	*P*21/*c*
a (Å)	10.8587 (4)	5.9948 (3)	10.1015 (6)
b (Å)	11.8492 (4)	8.8120 (6)	21.6426 (11)
c (Å)	12.7173 (5)	13.9547 (9)	11.7949 (7)
α (°)	69.065 (4)	91.627 (5)	90
β (°)	81.847 (3)	95.486 (5)	97.996 (5)
γ (°)	72.045 (3)	98.101 (5)	90
V ($Å^3$)	1452.93 (9)	725.82 (8)	2553.6 (3)
Z	2	2	4
ρ_{calc} (mg/mm^3)	1.268	1.520	1.484
μ (mm^{-1})	0.663	1.277	0.118
Total reflections	32,384	6096	17,389
Unique reflections	5496	2844	5727
GOOF (F^2)	1.052	1.027	1.009
R_{int}	0.0934	0.0298	0.0370
R_σ	0.0442	0.0370	0.0518
R_1 (all data)	0.0659	0.0549	0.0769
wR_2 (all data)	0.1614	0.1264	0.1027
R_1 ($\|F_o\| \geq 4\sigma_F$)	0.0512	0.0421	0.0478
wR_2 ($\|F_o\| \geq 4\sigma_F$)	0.1447	0.1106	0.0922

$R_1 = \Sigma||F_o| - |F_c||/\Sigma|F_o|$; $wR_2 = \{\Sigma[w(F_o^2 - F_c^2)^2]/\Sigma[w(F_o^2)^2]\}^{1/2}$; $w = 1/[\sigma^2(F_o^2)+(aP)^2 + bP]$, where $P = (F_o^2 + 2F_c^2)/3$; $s = \{\Sigma[w(F_o^2 - F_c^2)]/(n-p)\}^{1/2}$ where n is the number of reflections and p is the number of refinement parameters.

3. Results and discussion

Tautomeric forms of 1*H*-pyrrol-2,5-diimines and their derivatives (maleimides) were studied theoretically [27]. The existence of two tautomers of 2,3-diarylmaleimides is possible; the diketo tautomer (**A1**) and keto-enol tautomer (**B1**) are represented in Fig. 2.

According to the theoretical calculations, diketo **A1** tautomer of maleimide is the most stable both in the gas phase and in solution [27]. The labile hydrogen atom is attached to the nitrogen atom (**A1** in Fig. 2). Additional stabilization of the diketo form is accomplished by hydrogen bonds between two neighboring molecules in the solid phase [28]. We have studied the structures of 2,3-diarylmaleimides both theoretically and experimentally. It is known that **3a** crystalizes in two polymorphic forms, viz. α and β forms [28]. According to the XRD data [28], **α-3a** crystallizes in a triclinic crystal system, whereas packing of **β-3a** is monoclinic. The asymmetric unit of **α-3a** contains two molecules, whereas that of **β-3a** contains one molecule. The two N–H···O hydrogen bonds link the molecules pair-wise in both polymorphs of **3a**, thus forming the centrosymmetric dimers. The hydrogen bond distances in **α-3a** are 2.02 (3) and 1.99 (3) Å, while in **β-3a**, the hydrogen bond is shorter (1.91 (4) Å).

The prepared **3a** crystallizes in the triclinic space group *P*-1, which corresponds to **α-3a**.

Although, the crystals of **3b**–**d** were obtained analogously, **3b** and **3c** crystallize in the triclinic space group *P*-1, whereas **3d** crystallizes in the monoclinic space group *P*21/*c* (Table 1). In **3b**–**d**, two molecules are connected to each other by two hydrogen bonds (Figs. S1–S3 of Supporting Information). In the dimeric structure **3b**, the hydrogen bond lengths are 2.104 (2) and 2.069 (2) Å (Table 2S of Supporting Information). In the dimer **3c**, the two hydrogen bonds exhibit the same lengths (2.013 (2) Å) (Table 3S of Supporting Information). The hydrogen bond lengths in the dimer **3d** are 2.153 (2) and 1.965 (2) Å (Table 4S of Supporting Information). In **3d**, the additional weak C(O)···F interaction links two dimers. Owing to this intermolecular interaction, the orientations of dimers in two planes are observed and the crystallization in a monoclinic crystal system becomes more preferable.

The bond lengths C (1)=O (1), C (4)=O (2) (~1.20–1.23 Å), C (1)–N (1), C (4)–N (1) (~1.37–1.39 Å) are typical for the corresponding bonds in imides [28]. The C=O bond lengths lie in the double bond region. The C–N bond lengths are larger than the length of C=N double bond (~1.28 Å). The O (1)–C (1)–N (1), O (2)–C (4)–N (1),

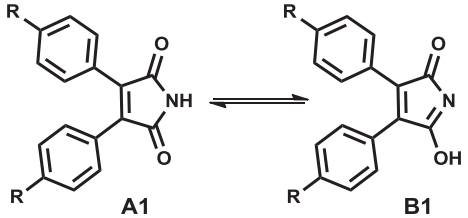

Fig. 2. Tautomers of 2,3-diarylmaleimides.

and C (1)–N (1)–C (4) angles in **3b**–**d** (125.0–126.2°, 124.1–125.6°, and 110.7–111.2°, respectively) are comparable to the appropriate previously published angles in **3a** [28]. According to the XRD data given above, 2,3-diarylmaleimides exist in the diketo tautomeric form in the solid state.

Accordingly to the DFT calculations, the diketo tautomer is stabilized by the dimer formation. The diketo tautomers of **3a**–**d** in the dimeric form have a comparatively lower relative energy than the single molecules of **3a**–**d** (~14 kJ mol^{-1}). Therefore, the diketo form is stabilizing by the dimerization in the solid state. Also, the stabilization of the diketo tautomer by the dimerization is possible in low-polar solvents. In the polar solvents, the stabilization of the diketo tautomer occurs by forming of hydrogen bond between the hydrogen atom H(N)$_{imide}$ and the basic atom of the solvent molecule. Such interaction is observed in the solvate of **3a** and 1-methylpyrrolidin-2-one [29].

The bond lengths and angles in the optimized structures of the dimers of **3a**–**d** are comparable with the XRD data. Larger differences are observed in the position of phenyls regarding to the maleimide ring. In all molecules, the rotation of the two phenyl rings with respect to the maleimide ring is due to steric interactions of the *ortho*-hydrogen atoms. In the calculated structures, the two phenyl rings are turned regarding the maleimide ring on the similar angle (~60°). In the solid state, the different angles between the corresponding ring planes (for example, 21 and 51° in **3b**) are because of the packing effects.

3,4-Diaryl-1*H*-pyrrol-2,5-diimines may exist in two tautomeric forms; the diimino form (**A2**) and imino-enamino form (**B2**) are represented in Fig. 3.

In 1*H*-pyrrol-2,5-diimines, the diimino form is also more stable than the imino-enamino form, however, the difference between the energies of tautomers is not so significant as in the case of maleimides [27]. Therefore coexistence of the diimino and imino-enamino tautomers in solution is possible. It is known that two 5-imino-3,4-diphenyl-1*H*-pyrrol-2-one molecules form centrosymmetric dimers via two N$_{pyrrole}$–H···N$_{imino}$ hydrogen bonds in the solid state [30]. The relative energy of 5-imino-3,4-diphenyl-1*H*-pyrrol-2-one in the dimeric form is lower than the energy of single molecule (ΔE = −18.5 kJ mol^{-1}) (pages S65, S69 of Supporting Information). In addition, we calculated the energy of dimer, where the two 5-imino-3,4-diphenyl-1*H*-pyrrol-2-one molecules link together by two N$_{pyrrole}$–H···O hydrogen bonds. The relative energy of this dimer is higher than the energy of dimer, where two molecules link together via two N$_{pyrrole}$–H···N$_{imino}$ hydrogen bonds (4.4 kJ mol^{-1}) (pages S69, S72 of Supporting Information). Insofar as 5-imino-3,4-diphenyl-1*H*-pyrrol-2-one is structurally related to 3,4-diaryl-1*H*-pyrrol-2,5-diimines, we suggested that diimino tautomers of 3,4-diaryl-1*H*-pyrrol-2,5-diimines can be stabilized by hydrogen bonding in the dimeric structure (Fig. 4).

We have evaluated the relative stability of the diimino tautomer of 3,4-di (4-methylphenyl)-1*H*-pyrrol-2,5-diimine, its dimer, and the imino-enamino tautomer. According to DFT calculations, the

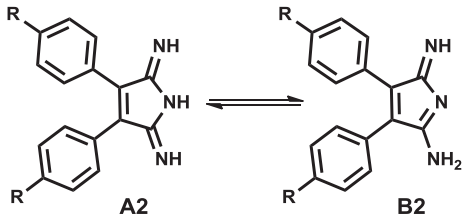

Fig. 3. Tautomers of 3,4-diaryl-1*H*-pyrrol-2,5-diimines.

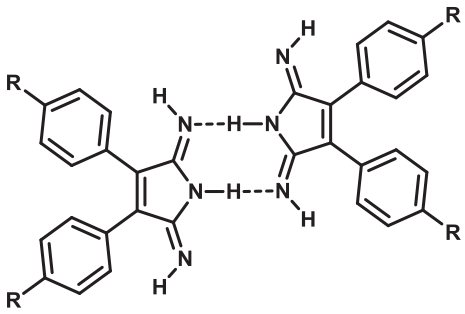

Fig. 4. Centrosymmetric dimer of 3,4-diaryl-1*H*-pyrrol-2,5-diimine.

dimer of 3,4-di (4-methylphenyl)-1*H*-pyrrol-2,5-diimine is more stable than the single molecule (ΔE = −17.9 kJ mol^{-1}). The difference between the total energies of imino-enamino and diimino tautomers of 3,4-di (4-methylphenyl)-1*H*-pyrrol-2,5-diimine is 7.8 kJ mol^{-1}.

To address the tautomerism, different types of the hydrogen-bonding motifs were designed and investigated recently [31–34]. For example, K. Epa et al. [32] have illustrated how relative stabilities of tautomers can drastically change with a change of environment and how, by controlling the environment, it is possible to deliberately isolate a desired tautomer. The metastable 1*H*-imidazo [4,5-b]pyridine tautomer can be selectively isolated by using urea derivatives as cocrystallizing agents capable to forming three hydrogen bonds. The average energy of the hydrogen bond C=O···H–N is ~48 kJ mol^{-1}. Also, the hydrogen bonds stabilize the nitrogen-linked conjugate 2-methyltetrazole-saccharinate in the 2*H*-2-methyltetrazole aminosaccharin tautomeric form [33,34]. Pairs of molecules are linked in dimers through intermolecular hydrogen bonds involving the NH spacer group as proton donor and the nitrogen in position 4 of the tetrazole ring as acceptor. The energy of the N$_{amino}$–H···N$_{tetrazole}$ hydrogen bond is estimated as ~14 kJ mol^{-1} by DFT calculations [34]. The hydrogen bonds in the 2,3-diarylmaleimide, 5-imino-3,4-diphenyl-1*H*-pyrrol-2-one, and 3,4-diaryl-1*H*-pyrrol-2,5-diimine dimers are relatively strong and comparable with those for other known dimeric structures. These intermolecular interactions stabilize the diketo tautomers of 2,3-diarylmaleimides, keto-imino tautomer of 5-imino-3,4-diphenyl-1*H*-pyrrol-2-one, and diimino tautomers of 3,4-diaryl-1*H*-pyrrol-2,5-diimines.

Two stable conformers (**C1** and **C2**) of 3,4-di(4-methylphenyl)-1*H*-pyrrol-2,5-diimine have been obtained by the geometry optimization (Fig. 5).

The relative energies are 0 and 5.3 kJ mol^{-1} for **C1** and **C2**, respectively.

The optimized structures of 3,4-di(4-methylphenyl)-1*H*-pyrrol-

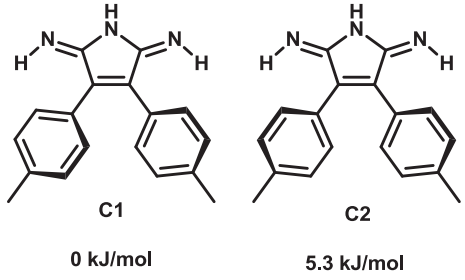

Fig. 5. Stable conformers (**C1** and **C2**) of 3,4-di (4-methylphenyl)-1*H*-pyrrol-2,5-diimine obtained by DFT calculations and their relative potential energies are indicated in units of kJ mol^{-1}.

2,5-diimine in the diimino and imino-enamino tautomeric forms, its dimer, 5-imino-3,4-di(4-methylphenyl)-1*H*-pyrrol-2-one, and 2,3-di (4-methylphenyl)maleimide with the bond lengths and angles are shown in Fig. S4.

The structures of the four 3,4-diaryl-1*H*-pyrrol-2,5-diimines and 2,3-diarylmaleimides (aryl = phenyl, 4-methylphenyl, 4-methoxyphenyl, and 4-fluorophenyl) have been optimized. It was found that the substituent at the 4th position of the phenyl ring slightly affects the bond lengths and the values of the valence angles in the pyrrole ring. Change of substituent has a little effect on the N–H bond order. Consequently, the acidity does not depend on the nature of substituent.

The schematic representations of the frontier molecular orbitals for **2b** and **3b** are exhibited in Fig. 6. The nature of the frontier MOs of compounds with different substituents (compounds **2a–d, 3a–d**) at the 4th positions of benzene rings is the same. The formation of dimers changes the HOMO and LUMO energies insignificantly. Also, dimers of 3,4-diaryl-1*H*-pyrrol-2,5-diimines and tautomeric forms (imino-enamino) have the same nature of the frontier MOs. The HOMO energies for 3,4-diaryl-1*H*-pyrrol-2,5-diimines and 2,3-diarylmaleimides are almost identical. While the LUMO energies for 3,4-diaryl-1*H*-pyrrol-2,5-diimines and 2,3-diarylmaleimides differ considerably (ESI). This is due to the contribution of heteroatom atomic orbital to LUMO. The HOMO energies for 3,4-diaryl-1*H*-pyrrol-2,5-diimines are almost independent on the substituent in the phenyl ring. However, the LUMO energies depend on the substituent stronger. The insertion of electron-withdrawing substituents leads to decreasing of frontier orbital energy. The differences between the frontier orbital energies $\Delta E_{HOMO-LUMO}$ for 2,3-diarylmaleimides are correlated with the fluorescence band shift value caused by the changing of substituent. This correlation was not found for 3,4-diaryl-1*H*-pyrrol-2,5-diimines due to a small band shift in the fluorescence spectra (Fig. 6).

For a deep insight into the optical properties of 3,4-diaryl-1*H*-pyrrol-2,5-diimines and 2,3-diarylmaleimides, UV–vis absorption and fluorescence emission spectra of these compounds in chloroform were calculated.

3.1. UV–vis absorption spectra and TD-DFT computational studies

The absorption spectra of 3,4-diaryl-1*H*-pyrrol-2,5-diimines and 2,3-diarylmaleimides in chloroform are shown in Fig. 7, and the corresponding spectroscopic data are listed in Table 2.

All pyrroldiimines display very similar absorption spectra with one or two intensive absorption bands in the near UV region. However, the absorption band of **2a** is shifted in the field of higher frequencies, compared with other pyrroldiimines. Use of methanol as a solvent causes a slight blue shift of the band at 278–311 nm accompanied with a decrease of its intensity.

The absorption spectra of 2,3-diarylmaleimides exhibit 4–6 bands (Table 2). The extinction coefficients of the bands at 240–253 nm are $0.9–1.1 \cdot 10^4$ M^{-1} cm^{-1}.

DFT and TD-DFT computational studies were performed to elucidate the electronic structures of the ground and excited states of **2a–f** and **3a–d**. The calculated UV–vis spectra for **2b** and **3b** are represented in Fig. S5. The calculated spectra are similar to the experimental spectra for these compounds. The ten transitions were calculated. The nature of vertical transitions for 3,4-di(4-methylphenyl)-1*H*-pyrrol-2,5-diimine is analyzed in Table 3.

The comparison of UV–vis spectra calculated for two conformations (**C1** and **C2**) of 3,4-diaryl-1*H*-pyrrol-2,5-diimines shows

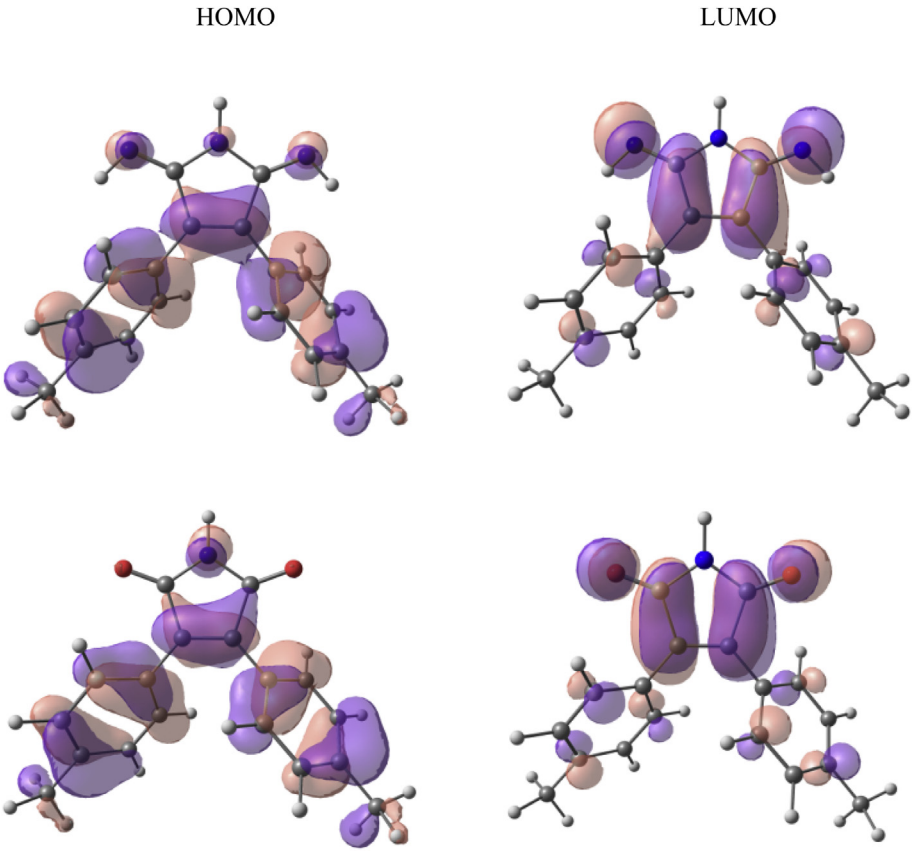

Fig. 6. Isosurfaces of MOs (HOMO and LUMO) for 3,4-di (4-methylphenyl)-1*H*-pyrrol-2,5-diimine (**2b**) and 2,3-di (4-methylphenyl)maleimide (**3b**).

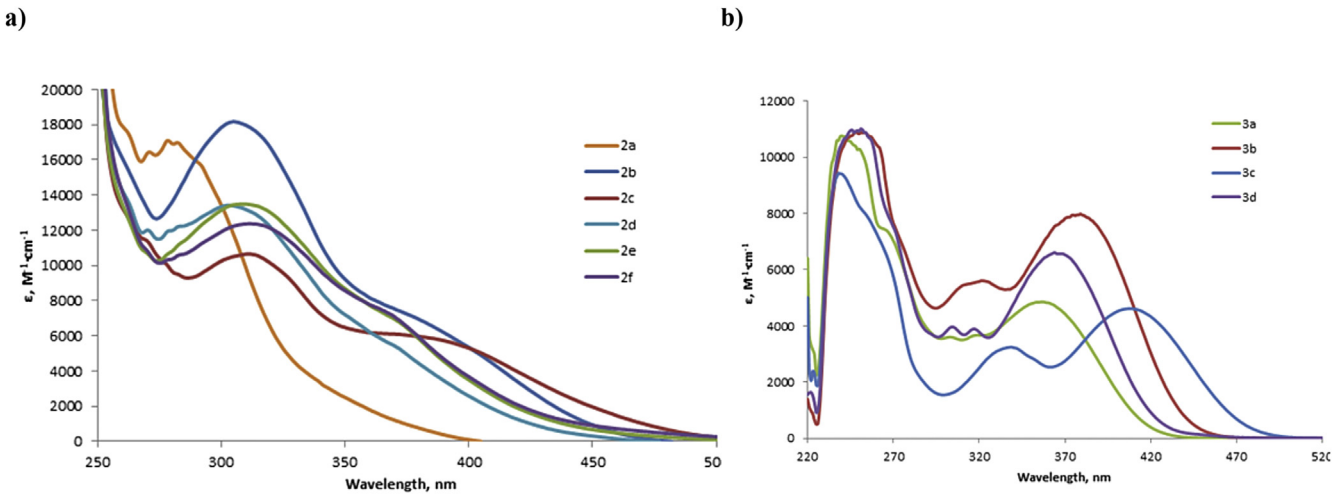

Fig. 7. The UV–vis absorption spectra of 3,4-diaryl-1*H*-pyrrol-2,5-diimines (a) and 2,3-diarylmaleimides (b) (C = $2.5 \cdot 10^{-5}$ M) in chloroform.

Table 2
The corresponding data of UV–vis absorption spectra in chloroform.

Compound	λ_{abs}, nm (ε, M^{-1} cm^{-1})
2a	278 (17,000)
2b	305 (18,000), 375[a]
2c	311 (11,000), 385[a]
2d	303 (13,000), 350[a]
2e	308 (14,000), 367[a]
2f	311 (12,000), 367[a]
3a	242 (11,000), 251 (10,000), 269 (7000), 304[a], 319[a], 357 (6000)
3b	253 (11,000), 262 (10,300), 280 (6000), 313[a], 325[a], 380 (8000)
3c	240 (9000), 257 (8000), 340 (3000), 409 (5000)
3d	252 (11,000), 273 (7000), 306[a], 318[a], 366 (7000)

[a] Shoulder.

that the nature of the transitions does not depend on conformation. However, the positions and intensities of the bands are very sensitive to the molecular conformation.

Most long-wavelength band has a high-frequency shift of 20 cm^{-1} and the simultaneous decrease in the relative intensity of the bands 1 and 2 in the spectrum of **C2** in comparison with that of **C1**. This is true for any type of substituent in the benzene ring.

On the other hand, the change of the substituent on the benzene ring has a little effect on the spectrum. The insertion of electron-withdrawing substituent (fluorine) leads to a slight shift (20 nm) of the long-wave band to the high frequency region.

According to the DFT-TD calculations of the long-wave band of the medium intensity (f = 0,17) for **2c** is due to the typical HOMO–LUMO transition, the second band is caused by the HOMO–1 – LUMO transition (f = 0.1).

The bathochromic shift of these transitions is due to a destabilizing contribution of oxygen p-orbital of methoxy group to the energies of HOMO and HOMO–1 orbitals (Table 3).

3.2. Emission spectra of 3,4-diaryl-1H-pyrrol-2,5-diimines

3,4-Diaryl-1*H*-pyrrol-2,5-diimines give the highest fluorescence intensity in the visible (blue) region upon excitation wavelength of 350 nm.

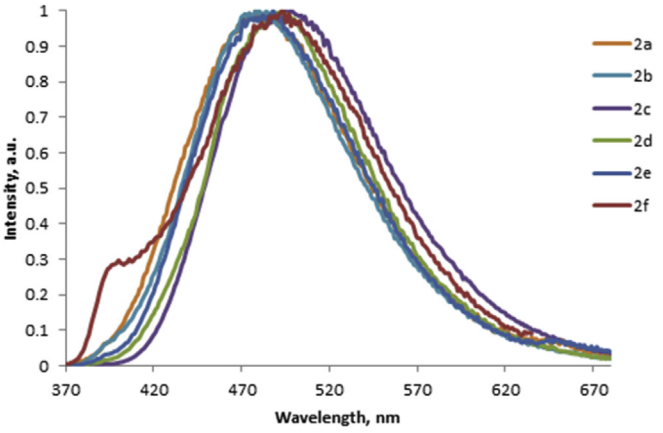

Fig. 8. Emission spectra of 3,4-diaryl-1*H*-pyrrol-2,5-diimines **2a**–**f** (C = $2.5 \cdot 10^{-5}$ M) in chloroform.

Table 3
The transitions in the UV–vis spectrum of **3b**.

№	MO[a]	Transitions	Assignment
1	73 → 74	HOMO → LUMO	$\pi(C(2)C(3)) - p_{\pi}^{+}(N_{imino}) + \pi(Ph,b_1) \rightarrow \pi^{a}(C(1)C(2)) - p_{\pi}^{-}(N_{imino})$
2	71 → 74	HOMO–2 → LUMO	$\pi(Ph,b_1) - \sigma(CC_{pyrrole}) - \pi(CH_3) \rightarrow \pi^{a}(C(1)C(2)) - p_{\pi}^{-}(N_{imino})$
3	70 → 74	HOMO–3 → LUMO	$\pi(Ph,a_2) + n^{-}(N_{imino}) \rightarrow \pi^{a}(C(1)C(2)) - p_{\pi}^{-}(N_{imino})$
4	72 → 74	HOMO–1 → LUMO	$p_{\pi}^{+}(N_{imino}) - p_{\pi}(N_{pyrrole}) \rightarrow \pi^{a}(C(1)C(2)) - p_{\pi}^{-}(N_{imino})$
5	69 → 74	HOMO–4 → LUMO	$\pi(Ph,a_2) + n^{+}(N_{imino}) \rightarrow \pi^{a}(C(1)C(2)) - p_{\pi}^{-}(N_{imino})$
6	68 → 74	HOMO–5 → LUMO	$n^{-}(N_{imino}) - \sigma^{-}(CC_{pyrrole}) \rightarrow \pi^{a}(C(1)C(2)) - p_{\pi}^{-}(N_{imino})$
7	66 → 74	HOMO–7 → LUMO	$n^{+}(N_{im}) + \sigma^{+}(\text{pyrrole ring}) \rightarrow \pi^{a}(C(1)C(2)) - p_{\pi}^{-}(N_{imino})$
8	73 → 75	HOMO → LUMO+1	$\pi(C(2)C(3)) - p_{\pi}^{+}(N_{imino}) + \pi(Ph,b_1) \rightarrow \pi^{a}(Ph,a_2)$
9	67 → 74	HOMO–8 → LUMO	$\pi^{-}(C(2)C(1)=N)_{pyrrole} \rightarrow \pi^{a}(C(1)C(2)) - p_{\pi}^{-}(N_{imino})$
10	73 → 78	HOMO → LUMO+4	$\pi(C(2)C(3)) - p_{\pi}^{+}(N_{imino}) + \pi(Ph,b_1) \rightarrow \pi^{a}(Ph,b_1)$

[a] MO is participated in the vertical transition (only orbitals with the highest coefficient in the linear combination are given for the transitions involving several MOs).

Table 4
Maximum excitation (λ_{ex}) and emission (λ_{em}) wavelengths and FL quantum yields (Φ) for **2a**–**f** in chloroform.

Compound	λ_{ex}, nm	λ_{em}, nm	Stokes shift, nm	Φ, %
2a	340	478	138	3
2b	341	478	137	16
2c	295[a], 348	494	146	17
2d	352[a], 370	493	123	7
2e	343	488	145	3
2f	348	493	145	3

[a] Shoulder.

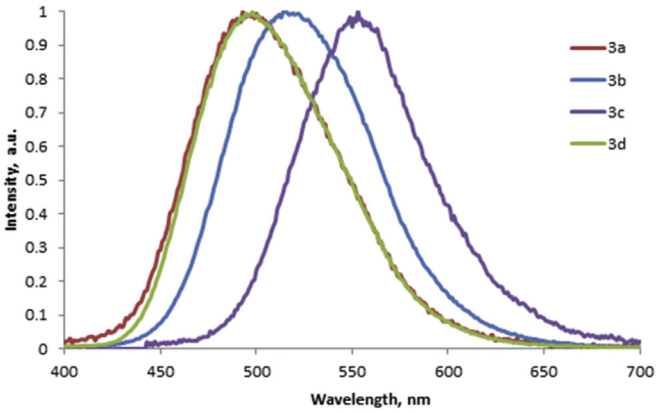

Fig. 9. Emission spectra of 2,3-diarylmaleimides **3a**–**d** (C = $6.25 \cdot 10^{-6}$ M) in chloroform.

The normalized fluorescence spectra of 3,4-diaryl-1*H*-pyrrol-2,5-diimines in chloroform are given in Fig. 8. Excitation and emission band maxima and fluorescence quantum yields are presented in Table 4.

The compounds **2a**–**c, e, f** have the broad excitation spectra with the strongest band at 340–348 nm.

Only one type of bands is observed in the luminescence spectra of 3,4-diaryl-1*H*-pyrrol-2,5-diimines in chloroform. This indicates the presence of one luminescence form in the solution. The insertion of donor substituents (CH_3O, CH_3) in the *para*-position of the benzene ring leads to increase of quantum yields of luminescence. The position of the maximum of luminescence band is practically independent on the substituents in the aromatic rings. All compounds are classified as fluorescent phosphors, because the short lifetimes of the excited states (≪0.1 m) are observed. **2a**–**f** display room temperature excited-state lifetimes between 2 and 13 ns?

The fluorescence spectra of 3,4-diaryl-1*H*-pyrrol-2,5-diimines in methanol exhibit similar spectral properties. The nature of the solvent does not affect the position and shape of the bands.

3.3. Emission spectra of 2,3-diarylmaleimides

The fluorescence spectra of 2,3-diarylmaleimides in chloroform have one intensive broad structureless band (Fig. 9).

The maxima of the spectra of H- and F-derivatives have the same position *viz.* 493–498 nm (Table 5). The donor substituents (Me, MeO) cause the bathochromic shift (**3b**: λ_{em} = 515 nm, red shift $\Delta\lambda$ = 22 nm; **3c**: λ_{em} = 553 nm, red shift $\Delta\lambda$ = 60 nm). The insertion of donor substituents leads to the increasing of the band intensity.

Table 5
Maximum excitation (λ_{ex}) and emission (λ_{em}) wavelengths for **3a**–**d** in chloroform.

Compound	λ_{ex}, nm	λ_{em}, nm	Stokes shift, nm
3a	365	493	128
3b	380	515	135
3c	433	553	120
3d	370	498	128

4. Conclusion

The geometry and electronic structure of 3,4-diaryl-1*H*-pyrrol-2,5-diimines and 2,3-diarylmaleimides were calculated by DFT B3LYP/6-31+G(d,p) method. We found that the substitution in 3,4-diaryl-1*H*-pyrrol-2,5-diimines and 2,3-diarylmaleimides has no effect on the molecular geometry. The substitution has a little effect on the electron density distribution and composition of frontier MOs. The UV–vis spectra of 3,4-diaryl-1*H*-pyrrol-2,5-diimines and 2,3-diarylmaleimides were interpreted. Fluorescence of 3,4-diaryl-1*H*-pyrrol-2,5-diimines and 2,3-diarylmaleimides were studied. The fluorescence spectra have large Stokes shifts. The insertion of donor substituents causes bathochromic shift of emission bands with hyperchromic effect. The effect of solvent on the emission spectra of 3,4-diaryl-1*H*-pyrrol-2,5-diimines and 2,3-diarylmaleimides is insignificant.

Acknowledgments

This research was supported by St. Petersburg State University (Grant 12.37.214.2016). We are grateful to Prof. V. Yu. Kukushkin (Saint Petersburg State University) for helpful discussions and insightful comments. We also thank the Centre for Optical and Laser Materials Research, Research Centre for X-ray Diffraction Studies, Educational Resource Centre of Chemistry, Centre for Chemical Analysis and Materials Research, and Centre of Magnetic Resonance (all belong to Saint Petersburg State University) for physicochemical measurements.

Appendix A. Supplementary data

Supplementary data related to this article can be found at 10.1016/j.molstruc.2017.06.048.

References

[1] C. Adachi, Third-generation organic electroluminescence materials, Jpn. J. Appl. Phys. 53 (2014) 060101–060111.
[2] M. Becuwe, D. Landy, F. Delattre, F. Cazier, S. Fourmentin, Fluorescent indolizine-b-cyclodextrin derivatives for the detection of volatile organic compounds, Sensors 8 (2008) 3689–3705.
[3] K.E. Sapsford, L. Berti, I.L. Medintz, Materials for fluorescence resonance energy transfer analysis: beyond traditional donor-acceptor combinations, Angew. Chem. Int. Ed. 45 (2006) 4562–4589.
[4] M. Nakazono, S. Nanbu, A. Uesaki, R. Kuwano, M. Kashiwabara, K. Zaitsu, Bisindolylmaleimides with large stokes shift and long-lasting chemiluminescence properties, Org. Lett. 9 (2007) 3583–3586.
[5] K. Saita, M. Nakazono, K. Zaitsu, S. Nanbu, H. Sekiya, Theoretical study of photophysical properties of bisindolylmaleimide derivatives, J. Phys. Chem. A 113 (2009) 8213–8220.
[6] T. Climent, R. Gonzalez-Luque, M. Merchan, Theoretical analysis of the excited states in maleimide, J. Phys. Chem. A 107 (2003) 6995–7003.
[7] H. Langhals, Cyclic carboxylic imide structures as structure elements of high stability. Novel developments in perylene dye chemistry, Heterocycles 40 (1995) 477–500.
[8] B.-C. Wang, H.-R. Liao, H.-C. Yeh, W.-C. Wu, C.-T. Chen, Theoretical investigation of stokes shift of 3,4-diaryl-substituted maleimide fluorophores, J. Luminescence 113 (2005) 321–328.
[9] W.-C. Wu, H.-C. Yeh, L.-H. Chan, C.-T. Chen, Red organic light-emitting diodes with a non-doping amorphous red emitter, Adv. Mater. 14 (2002) 1072–1075.
[10] C.-K. Tai, Y.-J. Lin, P.-L. Yeh, Y.-R. Tzeng, Y.-M. Chou, B.-C. Wang, Effects of substituent and solvent on the structure and spectral properties of maleimide derivatives, J. Mol. Struct. Theochem. 860 (2008) 58–63.
[11] H.-C. Yeh, W.-C. Wu, C.-T. Chen, The colourful fluorescence from readily-synthesised 3,4-diaryl-substituted maleimide fluorophores, Chem. Commun. (2003) 404–405.

[12] A.H. Cook, R.P. Linstead, Phthalocyanines. Part XI. The preparation of octaphenylporphyrazines from diphenylmaleinitrile, J. Chem. Soc. (1937) 929–933.
[13] M.N. Elinson, A.S. Dorofeev, S.K. Feducovich, P.A. Belyakov, G.I. Nikishin, Stereoselective electrocatalytic oxidative coupling of phenylacetonitriles: facile and convenient way to trans- and α– and β–dicyanostilbenes, Eur. J. Org. Chem. 18 (2007) 3023–3027.
[14] T.F. Baumann, A.G.M. Barrett, B.M. Hoffman, Porphyrazine binaries: synthesis, characterization, and spectroscopy of a metal-linked trinuclear porphyrazine dimer, Inorg. Chem. 36 (1997) 5661–5665.
[15] T. Furuyama, Y. Ogura, K. Yoza, N. Kobayashi, Superazaporphyrins: meso-pentaazapentaphyrins and one of their low-symmetry derivatives, Angew. Chem. Int. Ed. 51 (2012) 11110–11114.
[16] E. Bulatov, D. Boyarskaya, T. Chulkova, M. Haukka, 2,3-Diphenylmaleimide 1-methylpyrrolidin-2-one monosolvate, Acta Crystallogr. E 70 (2014) o260.
[17] C. Peifer, T. Stoiber, E. Unger, F. Totzke, C. Schaechtele, D. Marme, R. Brenk, G. Klebe, D. Schollmeyer, G. Dannhardt, Design, synthesis, and biological evaluation of 3,4-diarylmaleimides as angiogenesis inhibitors, J. Med. Chem. 49 (2006) 1271–1281.
[18] G.M. Sheldrick, A short history of SHELX, Acta Crystallogr. Sect. A 64 (2008) 112–122.
[19] O.V. Dolomanov, L.J. Bourhis, R.J. Gildea, J.A.K. Howard, H. Puschmann, OLEX2: a complete structure solution, refinement and analysis program, J. Appl. Crystallogr. 42 (2009) 339–341.
[20] CrysAlisPro, Agilent Technologies, Version 1.171.36.20 (Release 27 06 2012).
[21] A.D. Becke, Density-functional thermochemistry. III. The role of exact exchange, J. Chem. Phys. 98 (1993) 5648–5652.
[22] P.J. Stephens, F.J. Devlin, C.S. Ashvar, C.F. Chabalovski, M.J. Frisch, Theoretical calculation of vibrational circular dichroism spectra, Faraday Discuss. 99 (1994) 103–119.
[23] P.J. Stephens, F.J. Devlin, C.F. Chabalowski, M.J. Frisch, Ab initio calculation of vibrational absorption and circular dichroism spectra using density functional force fields, J. Phys. Chem. 98 (1994) 11623–11627.
[24] C. Lee, W. Yang, R.G. Parr, Development of the Colle-Salvetti correlation-energy formula into a functional of the electron density, Phys. Rev. B 37 (1988) 785–789.
[25] M.J. Frish, G.W. Trucks, H.B. Schlegel, et al., Gaussian 03, Revision D.01, Gaussian Inc., Wallingford CT, 2004.
[26] M.J. Frisch, G.W. Trucks, H.B. Schlegel, G.E. Scuseria, et al., Gaussian 09, Revision D.01, Gaussian Inc., Wallingford CT, 2010.
[27] A. Ackera, H.-J. Hofmann, R. Cimiraglia, On the tautomerism of maleimide and phthalimide derivatives, J. Mol. Struct. Theochem. 315 (1994) 43–51.
[28] A. Meents, H. Kutzke, M.J. Jones, C. Wickleder, H. Klapper, Polymorphs of 2,3-diphenylmaleic acid anhydride and 2,3-diphenylmaleic imide: synthesis, crystal structures, lattice energies and fluorescence, Z. Krist. 220 (2005) 626–638.
[29] E. Bulatov, D. Boyarskaya, T. Chulkova, M. Haukka, 2,3-Diphenylmaleimide 1-methylpyrrolidin-2-one monosolvate, Acta Crystallogr. E 70 (2014) o260.
[30] E. Bulatov, T. Chulkova, M. Haukka, 5-Imino-3,4-diphenyl-1H-pyrrol-2-one, Acta Crystallogr. E 70 (2014) o162.
[31] M. Juribasic, N. Bregovic, V. Stilinovic, V. Tomisic, M. Cindric, P. Sket, J. Plavec, M. Rubcic, K. Uzarevic, Supramolecular stabilization of metastable tautomers in solution and the solid state, Chem. Eur. J. 20 (2014) 17333–17345.
[32] K. Epa, C.B. Aakeroy, J. Desper, S. Rayat, K.L. Chandra, A.J. Cruz-Cabeza, Controlling molecular tautomerism through supramolecular selectivity, Chem. Commun. 49 (2013) 7929–7931.
[33] A. Ismael, J.A. Paixão, R. Fausto, M.L.S. Cristiano, Molecular structure of nitrogen-linked methyltetrazole-saccharinates, J. Mol. Struct. 1023 (2012) 128–142.
[34] A. Ismael, A. Gómez-Zavaglia, A. Borba, M.L.S. Cristiano, R. Fausto, Amino→imino tautomerization upon in vacuo sublimation of 2-methyltetrazole-saccharinate as probed by matrix isolation infrared spectroscopy, J. Phys. Chem. A 117 (2013) 3190–3197.